Science Bulletin 70 (2025) 825–828

Contents lists available at ScienceDirect

Science Bulletin

journal homepage: www.elsevier.com/locate/scib

Short Communication

Ab initio calculation of hyper-neutron matter

Hui Tong [a,*], Serdar Elhatisari [a,b,c], Ulf-G. Meißner [a,d,e,f,g]

[a] Helmholtz-Institut für Strahlen- und Kernphysik and Bethe Center for Theoretical Physics, Universität Bonn, Bonn, D-53115, Germany
[b] Faculty of Natural Sciences and Engineering, Gaziantep Islam Science and Technology University, Gaziantep, 27010, Turkey
[c] Interdisciplinary Research Center for Industrial Nuclear Energy (IRC-INE), King Fahd University of Petroleum and Minerals (KFUPM), Dhahran, 31261, Saudi Arabia
[d] Institute for Advanced Simulation (IAS-4), Forschungszentrum Jülich, Jülich, D-52425, Germany
[e] Center for Advanced Simulation and Analytics (CASA), Forschungszentrum Jülich, Jülich, D-52425, Germany
[f] Tbilisi State University, Tbilisi, 0186, Georgia
[g] Peng Huanwu Collaborative Center for Research and Education, Beihang University, Beijing 100191, China

ARTICLE INFO

Article history:
Received 6 November 2024
Received in revised form 14 December 2024
Accepted 20 December 2024
Available online 9 January 2025

In the era of multi-messenger astronomy, neutron stars arguably stand out as the most captivating astrophysical objects [1]. Neutron stars consist of the densest form of baryonic matter observed in the universe, and within their interiors, exotic new forms of matter may exist [2]. With the detection of various neutron star phenomena in recent years, such as gravitational waves and electromagnetic radiation, more valuable information regarding the mysterious dense matter within their cores will be unraveled. These findings, together with the measurements of the masses or radii, strongly constrain the neutron star matter equation of state (EoS) and theoretical models of their composition. However, the observation of neutron star masses above $2.0M_{\odot}$ has ruled out many predictions of exotic non-nucleonic components. Resolving this problem, known as the hyperon puzzle, is crucial for understanding the complex interplay between strong nuclear forces and the behavior of dense matter under extreme conditions [3,4].

In this study, we use the framework of nuclear lattice effective field theory (NLEFT) [5] to gain new insights into the generation of hyperons, more specifically $\Lambda(1116)$ particles, within dense environments. To enable calculations with arbitrary numbers of nucleons and hyperons, we introduce a novel formulation of the auxiliary field quantum Monte Carlo (AFQMC) algorithm, which allows for more accurate and efficient simulations free of sign oscillations using only one auxiliary field. Additionally, we incorporate two-body $N\Lambda$ and $\Lambda\Lambda$ interactions, as well as three-body terms such as $NN\Lambda$ and $N\Lambda\Lambda$, based on the minimal nuclear interaction [6], into the pionless effective field theory for nucleons. Initially, we focus on systems consisting solely of nucleons and determine the low-energy constants parameterizing the $2N$ and the $3N$ forces by constraining them to the saturation properties of symmetric nuclear matter, as it is well-known that fixing the $3N$ forces in light nuclei leads to a serious overbinding in heavier systems [7] if mostly local forces are employed. After constructing our interactions, we perform predictive calculations for the EoS of pure neutron matter (PNM) by considering up to 232 neutrons in a box to achieve densities up to five times the empirical saturation density of nuclear matter, i.e., $\rho = 0.8$ fm^{-3}. Our results for the EoS of PNM are in very good agreement with *ab initio* calculations using chiral interactions up to next-to-next-to-next-to-leading order (N3LO) [7] within the given density range. Subsequently, we introduce Λ-particles into our framework and determine the parameters of the $N\Lambda$ and $\Lambda\Lambda$ interactions by fitting them to experimental data, including the $N\Lambda$ cross section [8] and the $\Lambda\Lambda$ $^1S_0$ scattering phase shift from chiral effective field theory [9], respectively. The $NN\Lambda$ and $N\Lambda\Lambda$ forces are further constrained by the separation energies of single- and double-Λ hypernuclei, spanning systems from ${}^{5}_{\Lambda}$He to ${}^{6}_{\Lambda\Lambda}$Be, denoted as HNM(I). It is difficult to probe the behavior of the EoS at high densities encountered in neutron stars in terrestrial laboratories, and various phenomenological schemes [10] and microscopical models [3] suggest that hyperons emerge in the inner core of neutron stars at densities around $\rho \approx (2-3)\rho_0$. Therefore, similar to using the saturation properties of symmetric nuclear matter to pin down the three-nucleon forces (3NFs), we alternatively determined the $NN\Lambda$ and $N\Lambda\Lambda$ forces by the separation energies of hypernuclei and the Λ threshold densities $\rho_{\Lambda}^{\rm th}$ around $(2-3)\rho_0$ simultaneously in HNM(II) and HNM(III). We set $\rho_{\Lambda}^{\rm th}$ = 0.398(2)(5) and 0.520(2)(6) fm^{-3} for HNM(II) and HNM(III), respectively. In the next step, we perform simulations for hyper-neutron matter by including up to 116 hyperons in the box and calculate the corresponding EoSs. More details on the

* Corresponding author.
E-mail address: htong@uni-bonn.de (H. Tong).

https://doi.org/10.1016/j.scib.2025.01.008
2095-9273/

construction of the actions underlying PNM EoS and the three variants of hyper-neutron matter (HNM) are given in the Supplementary material.

The results for pure neutron matter and hyper-neutron matter are presented from our state-of-art nuclear lattice simulations. HNM is composed of neutrons and Λ hyperons, where ρ_N, ρ_Λ, and $\rho = \rho_N + \rho_\Lambda$ are the neutron, Λ hyperon and total baryon density of the system, respectively, and $x_\Lambda = \rho_\Lambda/\rho$ is the fraction of Λ hyperons. The Λ threshold densities $\rho_\Lambda^{\rm th}$ is determined by imposing the equilibrium condition $\mu_N = \mu_\Lambda$, where the chemical potentials for neutrons μ_N and lambdas μ_Λ are evaluated via the derivatives of the energy density $\varepsilon_{\rm HNM}$,

$$\mu_N(\rho, x_\Lambda) = \frac{\partial \varepsilon_{\rm HNM}}{\partial \rho_N}, \ \ \mu_\Lambda(\rho, x_\Lambda) = \frac{\partial \varepsilon_{\rm HNM}}{\partial \rho_\Lambda}, \tag{1}$$

which indicates that an accurate determination of the chemical potentials necessitates computing the energy density for various densities and different numbers of Λ hyperons.

In Fig. 1, the EoSs for PNM and for HNM are displayed. As anticipated, the inclusion of hyperons results in a softer EoS, and the threshold density is $\rho_\Lambda^{\rm th} = 0.325(2)(4)$ fm^{-3} for HNM(I). Here and what follows, the first (second) error is the statistical (systematic) one. This threshold aligns with predictions from various phenomenological schemes [10] and microscopical models [3], which suggest that hyperons emerge in the inner core of neutron stars at densities around $\rho \approx (2-3)\rho_0$. Furthermore, we construct two additional variants of HNM, denoted as HNM(II) and HNM(III). The EoS becomes stiffer at higher densities for these variants, indicating the inclusion of more repulsion in the three-body hyperon-nucleon interactions. The squared speed of sound, c_s^2, is also shown in the inset of Fig. 1. It is observed that the causality limit ($c_s^2 < 1$) is fulfilled for both PNM and HNM. It should be noted that in the pioneering calculations of Lonardoni et al. [4], they performed auxiliary field diffusion Monte Carlo (AFDMC) simulations with $N_n = 38, 54, 66$ neutrons and their PNM EoS is stiffer compared to our results and exceeds the causality limit for the speed of sound at densities above $\rho \simeq 0.68$ fm^{-3}. The EoS characterized by nucleonic degrees of freedom exclusively demonstrates a monotonic

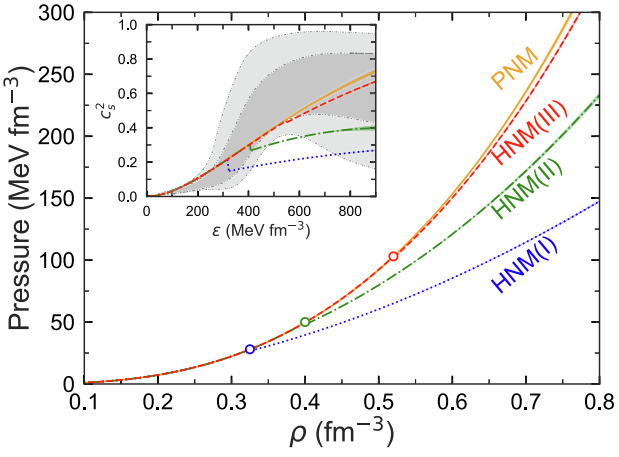

Fig. 1. EoS for HNM. The orange solid curve denotes pure neutron matter, obtained from the *NN* and *NNN* interactions. The red dashed line represents the EoS of HNM with hyperons interacting via the two-body interactions (*N*Λ and ΛΛ) and the third set of three-body hyperon-nucleon interaction (*NN*Λ and *N*ΛΛ). The blue dotted curve and the green dot-dashed curve are calculated with the first and second sets of three-body hyperon-nucleon interactions. The Λ threshold densities $\rho_\Lambda^{\rm th}$ are marked by open circles. In the inset, the speed of sound corresponding to the PNM and HNM EoSs is shown. The gray shaded regions are the inference of the speed of sound for neutron star matter in view of the recent observational data [11].

increase in c_s^2 with increasing energy density. The appearances of Λ hyperons, however, induce changes in this behavior, leading to non-monotonic curves that signify the incorporation of additional degrees of freedom. The onset of Λ hyperons precipitates a sharp reduction in the speed of sound, marking a significant transition in the stiffness of the EoS. For comparison, the constraints on c_s^2 within the interiors of neutron stars inferred by a Bayesian inference method are also shown [11]. These constraints are established based on recent multi-messenger data, in combination with limiting conditions from nuclear physics at low densities, as depicted by the gray shaded regions. The results for PNM and HNM(III) agree well with the marginal posterior probability distributions at the 95% and 68% levels. It should be noted that we used the minimal nuclear interaction, not the interactions derived from chiral effective field theory [7]. In Ref. [7], a full chiral interactions at N3LO was used for PNM and symmetric nuclear matter. This significantly increases the computational cost so that the calculations were done only at densities up to $2\rho_0$. In the future, we will incorporate the methodological advancements introduced in this work to explore neutron star EoS calculations using higher order chiral forces at densities larger than $2\rho_0$. While our calculations extend into the higher-density regime, we recognize that the behavior of EoS at these densities is less constrained, and the nuclear interaction we employ may introduce uncertainties. To validate the nuclear interaction in this work, we have quantified the theoretical uncertainty due to six different sets of three-nucleon forces which are shown in Fig. 1 and Fig. S2 (online). We find the theoretical uncertainty in Fig. S2 (online) is significantly smaller than the empirical uncertainty of the nuclear matter, and the uncertainty is also quite small for PNM in Fig. 1. This uncertainty quantification provides a solid foundation for future research on uncertainties in hyper-neutron matter, as the hyperonic three-baryon interactions used in our calculations follow the same uncertainty quantification approach. Therefore, the uncertainty in our nuclear interaction has been significantly reduced and is well controlled. Due to the current limitations of computational resources, calculating the EoS for arbitrary fractions of protons, neutrons, and other hyperons is still very challenging in any lattice approach. This can be achieved when more computational resources become available in the future and it will allow us to avoid the errors introduced by the so-called symmetry energy approximation.

The "holy grail" of neutron-star structure, the mass-radius (MR) relation, is displayed in Fig. 2. These relations for PNM and HNM are obtained by solving the Tolman-Oppenheimer-Volkoff (TOV) equations with the EoSs of Fig. 2. The appearance of Λ hyperons in neutron star matter remarkably reduces the predicted maximum mass compared with the PNM scenario. The maximum mass for PNM, HNM(I), HNM(II), and HNM(III) are $2.19(1)(1)M_\odot$,$1.59(1)(1)M_\odot$, $1.94(1)(1)M_\odot$, and $2.17(1)(1)M_\odot$, respectively. Three neutron stars have been measured to have gravitational masses close to $2M_\odot$: PSR J1614-2230, with $M = (1.908 \pm 0.016)M_\odot$ [15]; PSR J0348 + 0432, with $(2.01 \pm 0.04)M_\odot$ [16]; and PSR J0740 + 6620, with $(2.08 \pm 0.07)M_\odot$ [17]. These measurements significantly constrain the EoS of dense nuclear matter, ruling out the majority of currently proposed EoSs with hyperons from phenomenological approaches [18]. Our results show that the inclusion of the *NN*Λ and *N*ΛΛ interaction in HNM(III) leads to an EoS stiff enough such that the resulting neutron star maximum mass is compatible with the three mentioned measurements of neutron star masses. Therefore, the repulsion introduced by the hyperonic three-body interactions plays a crucial role, since it substantially increases the value of the Λ threshold density. It is also noteworthy that HNM (I) predicts a maximum mass above the canonical neutron star mass of $1.4M_\odot$, whereas the model (I) incorporating repulsive *NN*Λ interactions in the auxiliary field diffusion Monte Carlo [4],

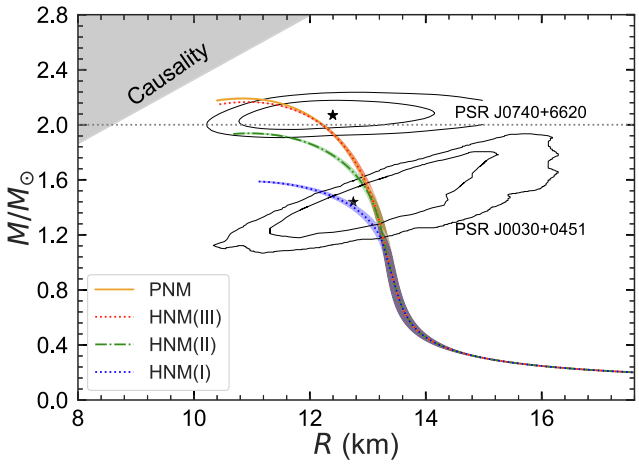

Fig. 2. Neutron star mass-radius relation. The legend is the same as of Fig. 1. The gray horizontal dotted line represents $2M_\odot$. The inner and outer contours indicate the allowed area of mass and radius of neutron stars by NICER's analysis of PSR J0030 + 0451 [12] and PSR J0740 + 6620 [13]. The excluded causality region is also shown by the grey shaded region [14].

Hartree–Fock [19], and Brueckner-Hartree-Fock (BHF) [3,20] calculations yield values below $1.4M_\odot$. In addition, the radii corresponding to PNM, HNM(I), HNM(II), and HNM(III) are $R_{1.4M_\odot} = 13.10(1)(7)$ km, $R_{1.4M_\odot} = 12.71(4)(13)$ km, $R_{1.4M_\odot} = 13.09(1)(8)$ km, and $R_{1.4M_\odot} = 13.10(1)(7)$ km, in order. Our results for the neutron star radii are also consistent with the constraints by NICER [12] for the mass and radius of PSR J0030 + 0451, i.e., mass $1.44^{+0.15}_{-0.14}M_\odot$ with radius $13.02^{+1.24}_{-1.06}$ km. The 68% and 95% contours of the joint probability density distribution of the mass and radius from the NICER analysis are also shown in Fig. 2. We further note that despite the significant reduction in the fraction of Λ hyperons caused by the hyperonic three-body force in HNM(III), they still exist within the interior of a $2.17M_\odot$ neutron star. This is different from the conclusion drawn in Ref. [4], where it was found the hyperonic three-body force in their parametrization (II) capable of generating an EoS stiff enough to support maximum masses consistent with the observations of $2M_\odot$ neutron stars results in the complete absence of Λ hyperons in the cores of these objects. We also note that while model HNM(III) successfully supports the mass of PSR J0740 + 6620 with $(2.08 \pm 0.07)M_\odot$, the $M(R)$ curve appears only marginally compatible with the combined experimental data. This issue is primarily associated with two factors. First, the characteristics of this neutron star mass region are predominantly determined by the EoS at higher densities. The baryon-baryon interactions considered in this work account only for contributions from the minimal interaction, whereas higher-order baryon-baryon interactions are expected to influence the EoS at higher densities. Therefore, it will be interesting and necessary to include the higher-order baryon-baryon interactions in the subsequent work. Second, the rotation of a neutron star induces corresponding increases in both its mass and radius, which can lead to a better agreement with the combined experimental data. The rotational frequency of this neutron star is 346 Hz, while the current calculations have been limited to static case. In the next step, we will incorporate the properties of rotating neutron stars.

In summary, we have performed the first lattice Monte Carlo calculation of hyper-neutron matter with a large number of neutrons and Λs and derived the resulting properties of neutron stars. In the next steps, one should include the proton fraction, other hyperons of the baryon octet, and make use of the recently developed high-fidelity chiral interactions at N3LO [7], though this will pose a formidable computational challenge.

Conflict of interest

The authors declare that they have no conflict of interest.

Acknowledgments

We are grateful for discussions with members and partners of the Nuclear Lattice Effective Field Theory Collaboration, in particular Zhengxue Ren. We are deeply thankful to Wolfram Weise for some thoughtful comments. Hui Tong thanks Jie Meng and Sibo Wang for helpful discussions. Serdar Elhatisari thanks Dean Lee for useful discussions on the auxiliary field formulations. We acknowledge funding by the European Research Council (ERC) under the European Union's Horizon 2020 research and innovation programme (AdG EXOTIC) (101018170), by the Ministerium für Kunst und Wissenschaft (MKW), Nordrhein-Westfalen (NRW) (NW21-024-A), and by Deutsche Forschungsgemeinschaft (DFG) (196253076) and National Natural Science Foundation of China (12070131001) through funds provided to the Sino-German CRC 110 "Symmetries and the Emergence of Structure in QCD". The work of Serdar Elhatisari was further supported by the Scientific and Technological Research Council of Turkey (TUBITAK project) (120F341). The work of Ulf-G. Meißner was further supported by Chinese Academy of Sciences (CAS) through the President's International Fellowship Initiative (PIFI) (2025PD0022).

Author contributions

The project was initiated and supervised by Ulf-G. Meißner. Serdar Elhatisari conceived the AFMC formulation for hypernuclear system, and code development, testing and optimization were led by Serdar Elhatisari with contributions by Hui Tong. Hui Tong performed the analysis of the data with contributions by Serdar Elhatisari, led production runs, and created the figures. All authors contributed to the writing.

Appendix A. Supplementary material

Supplementary data associated with this article can be found online at https://doi.org/10.1016/j.scib.2025.01.008.

References

[1] Abbott BP, Abbott R, Abbott TD, et al. GW170817: observation of gravitational waves from a binary neutron star inspiral. Phys Rev Lett 2017;119:161101.
[2] Lattimer JM, Prakash M. The physics of neutron stars. Science 2004;304:536–42.
[3] Schulze HJ, Rijken T. Maximum mass of hyperon stars with the Nijmegen ESC08 model. Phys Rev C 2011;84:035801.
[4] Lonardoni D, Lovato A, Gandolfi S, et al. Hyperon puzzle: hints from quantum Monte Carlo calculations. Phys Rev Lett 2015;114:092301.
[5] Lähde TA, Meißner UG. Nuclear lattice effective field theory: an introduction. Heidelberg: Springer; 2019. p. 957.
[6] Lu BN, Li N, Elhatisari S, et al. Essential elements for nuclear binding. Phys Lett B 2019;797:134863.
[7] Elhatisari S, Bovermann L, Ma YZ, et al. Wavefunction matching for solving quantum many-body problems. Nature 2024;630:59–63.
[8] Sechi-Zorn B, Kehoe B, Twitty J, et al. Low-energy lambda-proton elastic scattering. Phys Rev 1968;175:1735–40.
[9] Haidenbauer J, Meißner UG, Petschauer S. Strangeness $S = -2$ baryon–baryon interaction at next-to-leading order in chiral effective field theory. Nucl Phys A 2016;954:273–93.
[10] Weber F, Weigel MK. Baryon composition and macroscopic properties of neutron stars. Nucl Phys A 1989;505:779–822.
[11] Brandes L, Weise W, Kaiser N. Evidence against a strong first-order phase transition in neutron star cores: impact of new data. Phys Rev D 2023;108:094014.
[12] Miller MC, Lamb FK, Dittmann AJ, et al. PSR J0030+0451 mass and radius from *NICER* data and implications for the properties of neutron star matter. Astrophys J Lett 2019;887:L24.

[13] Riley TE, Watts AL, Ray PS, et al. A NICER view of the massive pulsar PSR J0740 +6620 informed by radio timing and XMM-newton spectroscopy. Astrophys J Lett 2021;918:L27.
[14] Lattimer JM, Prakash M. Neutron star observations: prognosis for equation of state constraints. Phys Rep 2007;442:109–65.
[15] Demorest P, Pennucci T, Ransom S, et al. Shapiro delay measurement of a two solar mass neutron star. Nature 2010;467:1081–3.
[16] Antoniadis J, Freire PCC, Wex N. A massive pulsar in a compact relativistic binary. Science 2013;340:6131.
[17] Fonseca E, Cromartie HT, Pennucci TT, et al. Refined mass and geometric measurements of the high-mass PSR J0740+6620. Astrophys J Lett 2021;915: L12.
[18] Burgio GF, Schulze HJ, Vidana I, et al. Neutron stars and the nuclear equation of state. Prog Part Nucl Phys 2021;120:103879.
[19] Dapo H, Schaefer BJ, Wambach J. On the appearance of hyperons in neutron stars. Phys Rev C 2010;81:035803.
[20] Wang SB, Tong H, Wang CC, et al. Tensor-force effects on nuclear matter in relativistic *ab initio* theory. Sci Bull 2024;69:2166–9.